Watershed Modelling in the Himalayan Region

Michael C. Quick * and Pratap Singh**
*Department of Civil Engineering
University of British Columbia
V6T 1Z4, CANADA
**National Institute of Hydrology
Roorkee (INDIA)

For rivers receiving flow from the Great Himalayan watersheds, the majority of the flow is generated from snowmelt and glacier runoff. This spring and summer runoff, comprising mostly snowmelt and glaciermelt, is the source of water for irrigation, hydroelectric power and drinking water supply. The monsoon rains only penetrate to the lower valleys, so that summer rain is a small contributor to total runoff. The majority of the precipitation input to these watersheds occurs as snow and falls during the mid to late winter period, caused by weather systems approaching from the west. Investigations to understand the snowmelt processes and snowmelt forecasting techniques are required for proper utilization of abundant water resources available in the Himalayan region.

In this study, the UBC Watershed Model is being calibrated for forecasting flows on the upper Satluj River system. This study has identified certain key issues which are central to achieving satisfactory forecasting results, and these issues are set out below.

(1)   Precipitation distribution. All watershed modelling depends on achieving an accurate estimate of precipitation distribution across the basin. In mountain regions there is a strong orographic pattern of precipitation which tends to be reasonably repeatable from year to year. Generally, precipitation increases at a certain rate with elevation and this rate can be estimated if there are sufficient data stations at various elevations in the basin. This data may be from standard meteorological stations with daily measurements of precipitation and temperature, or from snowcourse or snowpack measurements. If data is only available at

one or two locations, then precipitation gradients may have to be assumed and then modified by comparing computed and measured runoff from the watershed.

This iterative approach for determining precipitation gradients is only possible when dealing with snowmelt because snowmelt can be calculated from temperature which is also a function of elevation. There are therefore two definable constraints, firstly, the volume of runoff in the melt period and secondly, the snowmelt potential as a function of elevation. A third constraint is needed to be able to solve for the actual precipitation gradient, this third condition is the assumed form of the precipitation gradient. For example, if the gradient is assumed to be linear, or logarithmic, or some other functional form, then a unique solution can be found. Such a solution cannot be found for rainfall, and therefore it may be necessary to assume a similar gradient as for snow, or else much more data must be collected at different elevations to determine the gradient.

There are special problems with the orographic precipitation pattern in the northerly Himalayan watersheds, and these problems appear to be common for the whole region. The main feature of the precipitation is that the weather systems have to enter the region by crossing over high mountain barriers. On the upslope side of these barriers there is a strong increase of precipitation with elevation and much precipitation falls. However, on the lee side of the mountain barriers, which is the region under study, there is high precipitation at the high elevations, but, as the weather systems move in the downslope direction, there is a rapid decrease in precipitation. This decrease is typical of so-called subsidence zones and consequently valley precipitation can be quite small, and is frequently zero. This pattern of precipitation is a major difficulty for making accurate forecasts, because most data stations

are located at mid to lower elevations where precipitation is relatively low. Clearly, it is difficult to use these low values or even zero values of precipitation to estimate the much higher precipitation occurring at upper levels.

It should be noted that in another region of the Himalayas precipitation data was available for the weather side of the mountain barrier where the precipitation was much greater. This data proved to be a very good indicator of precipitation for the mountain peak region and the lee side, subsidence zone. That particular study (Quick and Pipes, 1989) clearly illustrates the value of using these high, upwind side precipitation measurements. In that particular study, the subsidence effect was so strong that valley precipitation in the northerly mountain region was essentially zero, so that estimating high elevation precipitation from the valley data was clearly impossible.

(2)   Temperature distribution. To estimate snowmelt, as will be discussed in a later section, it is necessary to estimate temperatures as a function of elevation in the watershed. Examination of measured temperatures at two elevations in the SPITI catchment indicates that lapse rates are quite variable, but fortunately somewhat systematic (Figure 1). In the winter, cold weather period quite high lapse rates of -10 to -14°C per km are observed. Such a high lapse rate is surprising, because anything in excess of -10°C per km, the dry adiabatic lapse, is unstable and should induce mixing. However these stations are separated horizontally by quite a number of kilometers, and perhaps the air mass temperature is modified by the time it reaches the valley region. Fortunately, the lapse rate during the melt season is much closer to the usual value of 6.4°C per km, which is the pseudo or saturated adiabatic lapse rate.

The watershed model has two methods for calculating temperatures as a function of elevation. One method computes temperatures using a variable lapse rate which is a function of the daily temperature range. Briefly, if there is a small daily range, the weather is probably cloudy and temperatures will decrease at the saturated adiabatic rate of 6.4°C/km. Alternatively, if the daily temperature range is large, then the weather is probably clear sky and temperatures will decrease at the dry adiabatic rate of -10°C/km.

The second method computes lapse rate using daily temperatures at a high and low station in the watershed. This method is very useful if the temperature stations are not too far apart horizontally, but in the present study the first method has proved better.

(3)   Melt seasons. Two distinct melt season periods need to be recognized, although they will be seen to overlap and interact to some extent. From April to June there is a snowmelt season which may extend to late June or even into July for heavy snow years. From June to September the glaciers become snow-free and glacial melt season contributes to runoff. These two seasons interact because in a heavy snow year, the glaciers will remain snow-covered for a longer time which will reduce glacial melt. Because the snow has a higher albedo, the snowmelt runoff will be less than the runoff that would occur from a snowfree glacier. In contrast, for a low snow year, the glaciers will be free of snow earlier, and although snowmelt will be less, there will be a greater contribution from the lower albedo glaciated regions. If the glaciated areas are significant, increased glacial runoff can therefore compensate to some extent for low snowpacks during a low precipitation year. The watershed model estimates snowpacks and computes when the glacial areas are snowfree. The model also computes albedo of the snowpack as the season progresses and these values

are used in the snowmelt routine, which will now be discussed.

As stated earlier, the upstream Himalayan streamflow runoff is dominated by snowmelt and glacier melt contributions. Because of the precipitation distribution discussed earlier, the majority of this snowmelt and glacier melt occurs at the higher elevations, about above 2000 m, and extending up to 5500 m or more. To estimate these snow and ice melt inputs, it is important to recognize the key factors which influence melt rates and thus it is necessary to use the meteorological data to model these processes with reasonable accuracy within the structure of the watershed model.

Snow and ice melt are caused by the following factors:

(1)   Incoming shortwave solar radiation is the fundamental energy input which drives the whole melt process.

(2)   Longwave radiation is generally a negative influence on melting, because melting snow is quite warm on an absolute temperature scale, and therefore radiates large quantities of heat energy back to the sky, behaving as a black body. The sky itself traps a fraction of both incoming shortwave and outgoing longwave and re-radiates longwave as a grey body, which has a radiation efficiency of about 75%.

(3)   Cloud cover has a large influence on both shortwave and longwave radiation fluxes. Shortwave radiation is intercepted by clouds and only a fraction, perhaps 10 to 25%, may penetrate to the ground surface, depending on cloud density. Longwave radiation balance is greatly influenced by clouds, because clouds radiate as black bodies, so that they greatly reduce the net negative longwave radiation. This cloud cover effect is easily observed under clear sky or cloudy conditions. Under clear

skies, temperature at night drops quickly and considerably, whereas with heavy cloud cover there may be very small night time temperature decrease.

Fortunately, these drastically different longwave energy balance situations can be easily characterized and estimated from air temperature measurements, because the daily temperature variation from maximum to minimum temperature will be a good indicator of cloud conditions. Furthermore, these cloud conditions, as indicated by the daily temperature range, will influence both the positive shortwave radiation melt contribution and the negative longwave energy loss which tends to decrease snow and ice melt.

4. <u>Convective heat transfer</u> is caused by the transfer of heat from the air mass to the snowpack or glacier. Convective heat transfer is very complex because it is a function of wind driven turbulent boundary layer processes and boundary roughness effects. Fortunately it is a smaller contribution to melt than the very important short and longwave radiation processes. The reason that convective heat transfer is less important is because the convective processes must overcome the buoyancy effect of warm air overlying a cold snow or ice surface. This buoyancy effect inhibits mixing of warm air downwards to the snow-ice surface and strong wind is needed to overcome this stability. Equations will be presented which estimate this convective heat transfer and it will be seen that the radiation components dominate.

5. <u>Advective heat transfer</u> is the term used to describe the heat flux associated with condensation on to the snow-ice surface or evaporation of moisture from the snow-ice surface. Because the latent heats of fusion and vaporization are so large, these

advective heat transfers are potentially significant. Like the convective heat transfer, these condensation-evaporation processes are controlled by complex boundary layer processes which are very difficult to estimate. Fortunately these processes are also limited by the stability effect of warm air over a cold surface, so that they only become important when winds are very strong.

6. Albedo, or reflectivity, is very important when estimating the net shortwave radiation energy input, but has no influence on the longwave radiant energy balance. The albedo effect is considerable because the albedo changes very considerably as the snow surface ages. New snow may reflect as much as 95% of the incoming shortwave radiation, whereas old snow may have an albedo as low as 0.4 and glacial ice has an albedo typically of about 0.3. Consequently a glacial surface can absorb twelve times as much shortwave energy as is absorbed by very fresh snow. More realistically, snow may quickly age to an albedo of 0.6, and compared with glacier ice, will only absorb half as much solar energy. Clearly it is very important to estimate how the albedo changes during the melt season, and a method will be outlined for calculating albedo as a function of cumulative melt, but modified by any new snow which may fall.

7. Exposure and aspect. It is well known that northern or southern aspect and site exposure can have a big influence on snow and ice melt. A clear indication is given by the glacier development in sheltered valleys on north facing slopes and by the delayed snowmelt on northern aspects. In calculating the shortwave radiation inputs, it is therefore important to allow for the orientation of the mountain slopes and the surrounding elevation angle of the mountain barrier which determines the local

sunrise and sunset.

To examine the influence of aspect and barrier height, a mathematical computer model was used to integrate the solar radiation input as a function of time of year. In the winter and up to late April, it was found that north facing slopes receive significantly less radiant energy. However, perhaps surprisingly, during the peak snowmelt months of May, June and July, the elevation is so high and the sun rises and sets so far to the north that north facing slopes receive nearly as much solar energy during the whole day as a south facing slope. Also it was found that east and west facing slopes receive quite similar radiation to a south facing or flat slope. Barrier height had a significant effect on all these radiation values, because sunrise was delayed and sunset occurred sooner. Using this model, a set of seasonal correction factors was estimated for various slopes, aspects, and barrier heights. Because of the complex geometry of mountain regions, it is not feasible to characterize the whole region in detail, but the results of the study slowed that a reasonably representative set of factors could be determined for the north and south facing slopes. The east and west facing slopes could be considered as similar to the south facing orientation.

Snowmelt Equations

The only data available for the estimation of snowfall and snowmelt is usually daily precipitation and temperature data, maximum and minimum. The following equations have been developed and extensively tested for estimating the various snowmelt components in mountain watersheds.

SIMPLIFIED ENERGY COMPONENTS

(a) Net Shortwave - Energy Input

$$Melt = I_S \left(1 - C_L\right) \left(1 - A_L\right) \, mm/day \tag{1}$$

where C_L is cloud cover, A_L is the albedo of the snowpack and I_S is the incident solar radiation, which varies seasonally and with latitude and with atmospheric conditions. At 35° North, I_S can be expressed in terms of millimeters of melt equivalent per day instead of Langleys per day,

$$I_S = 54 - 29 \cos \frac{2\pi N}{365} \, mm/day \tag{2}$$

The albedo and cloud cover reduce the potential melt values of equation (2) to the net values expressed by equation (1).

(b) Longwave Radiation

Stefan's law can be expanded in terms of the temperature above freezing, T, so that the longwave black body radiant energy, I_L, can be expressed as a linear function of temperature plus small higher order terms,

$$
\begin{aligned}
I_L &= \sigma \left(273 + T\right)^4 \, Langleys/day \\
&= \sigma \cdot 273^4 \left[1 + \frac{4T}{273} + \frac{6T^2}{273^2} + \ldots\right] \\
&= 661(1 + 0.015\,T + 0.0001\,T^2 + \ldots \\
&= 82 \cdot 6\,(1 + 0.015\,T + \ldots) \, mm/day
\end{aligned}
\tag{3}
$$

209

Under clear sky conditions in an open, tree free area, the net longwave radiation received by the melting snowpack is the difference between the black body radiation from the 0°C snowpack and the incoming grey body radiation from the clear sky. Various estimated values for the grey body radiation are available, some of which are quoted in the U.S. Corps Snowmelt Report (1955). All of the equations show a small dependence on humidity of the atmosphere, such as equations due to Brunt and Angstrom. The simplest equation, from the Lake Hefner study, is

$$I_{LA} = \sigma T^4 \left(0.749 + 0.0049\, e_a\right) \ Langleys/day \tag{4}$$

where I_{LA} is the atmospheric longwave radiation, and e_a is he vapour pressure in millibars. The dependence on vapour pressure is so small that it is reasonable to accept the value,

$$I_{LA} = 0.757\, \sigma T^4 \tag{5}$$

The net clear sky incoming longwave radiation, I_{LN}, can therefore be written, using the linearization of Equation (3),

$$I_{LN} = 661 \left[0.757\left(1 + 0.015\, T_A\right) - \left(1 + 0.015\, T_S\right)\right] \ Langleys/day \tag{6}$$

where T_A is mean air temperature and T_S is the snow surface temperature, which is zero for a melting snowpack. Therefore,

$$I_{LN} = 7.51\, T_A - 161 - 9.92\, T_S \ Langleys/day \tag{7}$$

210

In snowmelt equivalent,

$$I_{LN} = 0.94 \, T_A - 20.1 - 1.24 \, T_S \quad mm/day \tag{8}$$

For a melting snowpack, T_S is zero, and I_{LN} does not become positive until T_A exceeds 21.4°C.

(c) <u>Net Longwave under Cloud Conditions</u>

Clouds, temperature, T_C, act as black bodies, so that under 100% cloud cover, the net incoming longwave, I_{LNC}, is

$$
\begin{aligned}
I_{LNC} &= 9.92 \left(T_C - T_S \right) \quad Langleys/day \\
&\approx 1.24 \left(T_C - T_C \right) \quad mm/day
\end{aligned}
\tag{9}
$$

The clear and cloudy sky equations are combined into an expression for the net longwave exchange, I_{LNT}, for a partial cloud cover fraction, C, so that, for a melting snowpack at 0°C,

$$I_{LNT} = \left(0.94 \, T_A - 20.1 \right) (1 - C) + 1.24 \, T_C \cdot C \quad mm/day \tag{10}$$

The cloud temperature can often be approximated by the dew point temperature, which is approximately the minimum air temperature.

(d) <u>Convective and Advective Heat Transfer</u>

The U.S. Corps Report (1955) and Anderson (1976) present equations for convective and advective heat transfer. Anderson refers to the question of air mass stability, but does not incorporate the results into a final relationship. The following equations are an approximate estimation of the net heat transfers which have been developed from the earlier

211

work.

Under neutrally stable conditions the convective heat transfer, Q_C, is approximately,

$$Q_C = 0.113 \left[\frac{p}{101}\right] T_A \cdot V \quad mm/day \tag{11}$$

in which p is the atmospheric pressure in kN/m^2 for the elevation being considered, T_A is the mean air temperature and V is the wind speed in kilometers per hour.

Similarly, the advective, or condensation, melt Q_A under neutrally stable conditions is approximately,

$$Q_A = 0.44 \, T_d \cdot V \quad mm/day \tag{12}$$

where T_d is the dew point temperature, which can be approximated by the minimum air temperature.

Both the convective and advective melt rates are reduced by a factor R_M which is a function of the bulk Richardson number R_I. A linearization of R_M, subject to the limitations given below, is

$$R_M = 1 - 7.7 \, R_I \tag{13}$$

where

$$R_I = \frac{2_g \cdot Z_A \, T_A}{\left(T_A + 273\right) V^2} \approx 0.095 \, \frac{T_A}{V^2} \tag{14}$$

where V is the wind speed at a reference height Z.

This linearization is reasonable for R_I between +0.12 and -0.1. For positive air temperatures, R_M increases to about 1.8 and then slowly goes a little higher.

This R_M factor is based on idealized laboratory conditions. In steep mountain terrain, our own studies of snowmelt indicate that stability is greatly reduced by "terrain mixing" caused by large scale roughness and slope. Consequently R_M may increase by as much as a factor of 2.5 times, which can be considered to incorporate an additional "terrain mixing" factor.

(e)   Rainmelt

Snowmelt from rain MBR is computed as follows:

$$BMR = K \cdot TM \cdot RN \quad mm/day \tag{15}$$

where K = a constant, and RN = rainfall.

This formula assumes that the rain falls at the mean temperature and the K factor (mm of melt/°C of rain above zero) represents the heat content of the rain.

APPLICATION OF THE SIMPLIFIED ENERGY SNOWMELT EQUATIONS

There are advantages to be gained from using energy equations for calculating snowmelt. The physical basis of the equation makes it possible to estimate snowmelt for forested and open conditions, for clear or cloudy weather, for various slope and aspects of mountainous watersheds and for changes in elevation. It is also possible to argue the impacts of changing forest cover or the snowmelt that would be experienced under extreme and unusual weather sequences.

For most high mountain regions data on radiation, cloud cover, etc., are not available. The factors which must be described are the cloud cover, albedo, wind, cloud temperature and dew point temperature. All other factors can be estimated from known physical

213

behaviour. As reasonable approximations, it has been found possible to represent these various factors with temperature-based estimates.

(a) Cloud Cover

The cloud cover has been assumed to be related to the daily temperature range,

$$\left(1 - C_L\right) = \frac{\left(T_{MAX} - T_{MIN}\right)}{D_R} \tag{16}$$

in which C_L is the cloud cover fraction, T_{MAX}, T_{MIN} are the daily maximum and minimum temperatures, and D_R is the daily temperature range for open sky conditions at a certain elevation in the watershed.

(b) Wind Estimate

The wind tends to produce a decrease in daily temperature range, so that cloudy conditions are also windy conditions.

$$V = K_R \left(T_{MAX} - T_{MIN}\right)^{-1/2} - K_v \tag{17}$$

in which K_R and K_v vary slightly with elevation.

(c) Albedo

The albedo is modelled by three relationships. Fresh snow is assumed to settle and change its albedo from a starting value of 0.9, which then decays by a factor of 0.9 per day until it reaches a settled value, A_{LS}, of 0.65, i.e.,

$$A_{LS(j+1)} = 0.9 \, A_{LS(j)} \tag{18}$$

in which $A_{LS(0)}$ starts at 0.9 and $A_{LS(j+1)}$ is greater than or equal to A_{LS}, usually 0.65.

From then on, the albedo continue to decrease at an exponential decay rate, which is controlled by the calculated cumulative melt for the season, given by

$$A_{Lj} = A_{LS} \, e^{\frac{-\sum M}{K_L}} \tag{19}$$

where A_{LS} is the settled value, usually 0.65, $\sum M$ is the cumulative seasonal melt in millimeters and K_L is a constant, approximately of the order of the total seasonal melt, usually taken as 4000 mm.

When new snow occurs, if it is greater than 25 mm, the albedo is assumed to return to a value of 0.9. The albedo then decays again at the 0.9 rate, specified by Equation (18), but continued down until it reaches the value computed on the day before the snow occurred, A_{Lj} from Equation (19). The underlying recession described by Equation (19) then takes over. This process allows a fairly rapid change of albedo from 0.9 to 0.65, or down to the calculated A_{Lj} value from Equation (19), and then a slow recession as the season advances to albedo values of 0.4 or even 0.3 for very deep and aged snowpacks, when it becomes free of snow, is assumed to have an albedo of 0.3

These relationships for cloud cover, wind and albedo have been developed using SIHP (1986, 87, 88) data gathered in the Himalayas and also using U.S. Corps. of Engineers (1952) data gathered in great detail for the Central Sierra Snow Studies as discussed by Quick (1987).

215

The user must supply the following information:

1. the temperature range which controls cloud cover specified by the parameter AφFOGY, AφSUNY, AφFOGFX, where AφFOGX is the maximum range for a station, AφFOGY is the range below which complete cloud cover exists, and AφSUNY is the range above which the sky is assumed clear.

    This temperature range depends on the elevation of meteorological stations and decreases as elevation increases. Typical values are specified in the calibration parameter fields for the various watersheds.

2. the percentage of forested and open area.

3. the aspect: the area and slope of north and south facing regions of the watershed and the topographic barrier height at sunrise and sunset.

WATERSHED MODELLING OF THE SPITI CATCHMENT

The Spiti watershed is tributary to the Satluj River system and has an area of 10071 km^2. The watershed is located to the north of the Great Himalayan divide and extends into Tibet. The elevation mainly ranges from 2900 m to 5600 m but with a small area extending to a peak of 7026 m. Half of the basin is oriented to the north-east and half to the south. The glaciated area is small, of the order of about 5% of total catchment area, but even so this glaciated area is significant in the late season melt. The mean seasonal and mean monthly precipitation distribution are shown in Figure 2 and Figure 3, respectively, can be seen that most precipitation falls as snow in the winter period, peaking in March, and results from westerly weather systems (Figure 2). The monsoon has little influence on this

216

watershed, except for the occasional summer rainstorm.

The Spiti River joins the main Satluj which flows west from Tibet. The Spiti covers about two-thirds of the Indian part of Satluj basin in which snow occurs and is also a higher yielding watershed.

There is a good database with a number of precipitation stations. For this study the two main meteorological stations have been used because both temperatures and precipitation are measured manually on a year round basis. These stations cover a good range of elevations from Namagia at 2910 m to Kaza at 3639 m. Only precipitation data is measured at Lossar, but this station is useful because it is at the highest elevation of all the stations, at 4071 m. It would be useful to have data even higher in the watershed, because the analysis indicates that precipitation increases .,. e steeply above the Lossar elevation.

Previously Mohile et al. (1988) carried out a study to develop a regression relationship between temperature of Kaza and snowmelt runoff collected at a proposed dam across Spiti river 4 km upstream of Kaza in this basin. The extension of discharge data at the proposed dam site was made based on this relationship. Efforts were also made to develop a relationship between discharges of Kaza and Namgia in the same basin.

OPERATION OF THE UBC WATERSHED MODEL

For the present work, results will be presented for three hydrologic years of data, from October 1987 to September 1990. The UBC Watershed Model uses inputs of daily temperature and precipitation and from these inputs the model then estimates the seasonal accumulation and melting of the snowpack. The melted snow and rainfall are then routed

through a system of storage routing reservoirs which represent the watershed storage effects and the outflows are then combined to give estimates of the daily streamflow. The measured streamflow is not used directly in the calculations but is used as reference data to test the accuracy of the flow estimates. The results presented in Figures 4 to 6, therefore depend entirely on the input meteorological data, which in this instance is the daily record of temperature and precipitation. The Figures 4 to 6 show plots of the measured flow, the computed and the estimated groundwater flow component. Examination of these figures indicates that there are several different time scales of watershed response, ranging from a very fast response which occurs within the day to a very slow groundwater response which delays runoff for many months. This slow groundwater flow can be observed during the long winter recessional flow period.

Figure 7 shows a plot of the estimated snowpack water equivalent in millimeters for the year 1988-89. It can be seen that the snowpack builds up during the winter period, reaching a maximum in March or April. Generally April to July there is melting of the snowpack in response to the high solar radiation and the associated warm air temperatures. The seasonal snowcover is melted by late June or July, and further melt then occurs from the snowfree glaciated areas. This rapid melting is computed from the equations presented earlier and is clearly indicated by the rapid reduction of snow water equivalent.

Figure 8 shows the computed values of the albedo of the snowcover for a particular elevation zone. It can be seen that the winter snowcover has a high albedo, so that only a small fraction of the incoming solar radiation is absorbed by the snowpack. Consequently melt rates are low at the start of the season. As the melt season progresses, the snow crystal

218

structure changes because of freeze-thaw cycling which causes the albedo of the snow to reduce. Figure 8 indicates a gradual reduction in albedo from 0.9 to value of 0.5 or less. When new snow falls, the albedo increases again to that of new snow, but after more melt occurs, the albedo returns to its previous lower value. This albedo modelling is an important aspect of the estimation of snowmelt because if albedo changes from 0.9 to 0.6 the melt rate will increase by a factor of about four. A snowfree glaciated surface can typically have an albedo of 0.3, so that the melt rate can then be seven times greater than new snow, and twice as high as a snowpack with an albedo of 0.6, which is typical of a moderately aged snowpack.

During the calibration process it was found that Kaza precipitation and temperature data was the most representative. Kaza receives an annual precipitation which is close to the average annual streamflow runoff depth which for a six year period was 439 mm/annum compared with Kaza average precipitation for the same period of 463 mm. The Kaza data was therefore used to compute precipitation and melt for the elevation bands between 4400 m and 6000 m.

Namgia temperatures are warmer than Kaza, even allowing for a normal temperature lapse rate of 6.4°C/km. Namgia precipitation is also lower, but is more representative for the valley region. Namgia temperature and precipitation data was therefore used for the two lowest elevation zone between 3500 m and 4100 m.

As discussed earlier, the recorded average annual precipitation at the three stations is shown in Figure 2. On the same graph is plotted the average annual precipitation which is computed using the watershed model gradients as calibrated to match the observed runoff

runoff on a daily basis. From this graph, it is seen that the model computes about the same precipitation as Kaza and Namgia, less than Lossar and a steep increase above 5200 m. This steep increase in precipitation at the high elevation is a strong argument for installing high elevation data stations, or at least measuring snowpack water equivalent in April or May to check the computed values.

Examination of the observed and calculated streamflow presented in Figures 4 to 6 indicates that the general hydrograph shape is quite well represented. In 1987-88 the early runoff is under-estimated until mid-June. The peak flow is slightly over-estimated, but the period from July to September is reasonably estimated. In 1988-89, the early season in May is slightly underestimated, but the rest of the runoff season is well estimated for volume and shape except for one peak in which rain is probably a factor. Summer rain can be variable in extent and may not be measured with any accuracy. In 1989-90, the total hydrograph is quite well estimated, even the short-term shape is good.

The key issue in watershed modelling is to determine the basinwide distribution of precipitation. Mountain watershed modelling is possible because the mountain precipitation tends to follow a repeatable orographically determined pattern, so that even one or two reliable data stations, if they are situated high enough in the watershed, can be good indicators of basin precipitation. Valley precipitation is unreliable because no precipitation may be recorded even when considerable precipitation is falling at high elevations.

CONCLUSIONS

The results presented confirm that it is reasonable to assume that mountain precipitation pattern is predictable and falls in a repeatable pattern from year to year. Three years is a small test but is a promising start. Further testing is necessary because in some regions there are different patterns of precipitation from year to year depending on variations in the direction of approach of the weather systems. If this variation in weather system can be identified, it is still possible to model for such situations.

snowmelt and glacier melt are more forecastable than rain because snowpacks are built up during a whole season and measured cumulative precipitation is usually a good statistical representation of the snowpack. The snowmelt and glacier melt can be reliably calculated from an energy budget method using daily maximum and minimum temperatures as basic input data.

The snowmelt estimates and the measured streamflow can be used in combination to determine precipitation gradients, and this is a further advantage of snowmelt studies in contrast to rainfall runoff. These analyses indicate very large increases of precipitation at high elevations and give emphasis to the hydrological importance of these high mountain regions which feed both snowmelt and glacier development.

In basins where glaciers are significant, perhaps 5% of the basin area or greater, the glaciers from a valuable melt contribution, especially during low snowpack years. In high snowpack years, the snowcover on the glaciers reduces glacial melt, preserving the glaciers for their valuable contribution in the drought years.

ACKNOWLEDGEMENTS

REFERENCES

Anderson, E.A. (1976), "A point energy and mass balance model of a snow cover," NOAA Tech. Report, NWS 19, National Weather Service, U.S. Dept. of Commerce.

Mohile, A.D., Rao, P.R., Sood, S.C., and Dhillon, M.S. (1988), "Snowmelt, its estimation and forecasting," 54th R&D Session of CBIP, 30th April - 3rd May, 1988, Ranchi, Bihar, India, pp. 167-172.

Quick, M.C. (1987), "Snowmelt hydrology and applications to runoff forecasting," National Lecture, sponsored by Associate Committee on Hydrology of National Research Council and Hydrotechnical Committee of the Canadian Society of Civil Engineers.

Quick, M.C. and Pipes, A. (1989), "High Mountain Runoff and Applications to Runoff Forecasting," Proceedings of the Canadian Society of Civil Engineers Annual Conference, St. Johns, Newfoundland, pp. 232-247.

S.I.H.P. Snow and Ice Hydrology Project, Annual Reports, Wilfred Laurier University, Waterloo, Ontario, Canada, 1986, 1987, 1988.

U.S. Corps (1952), "Hydrometeorological log of the Central Sierra Snow Laboratory, 1948-49, South Pacific Division, Corps of Engineers, U.S. Army, San Francisco.

U.S. Corps of Engineers (1955), "Lysimeter Studies of Snowmelt, Snow Investigations, Research Note 25, North Pacific Division, Portland, Oregon, pp. 1-41.

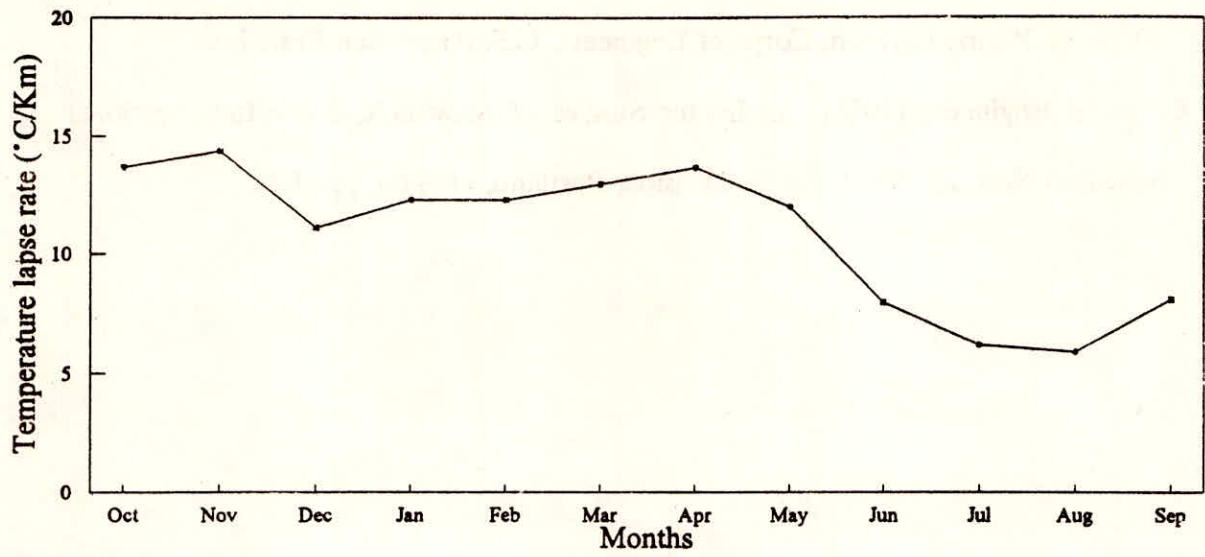Figure 1 : Mean monthly temperature lapse rates between Namgia and Kaza

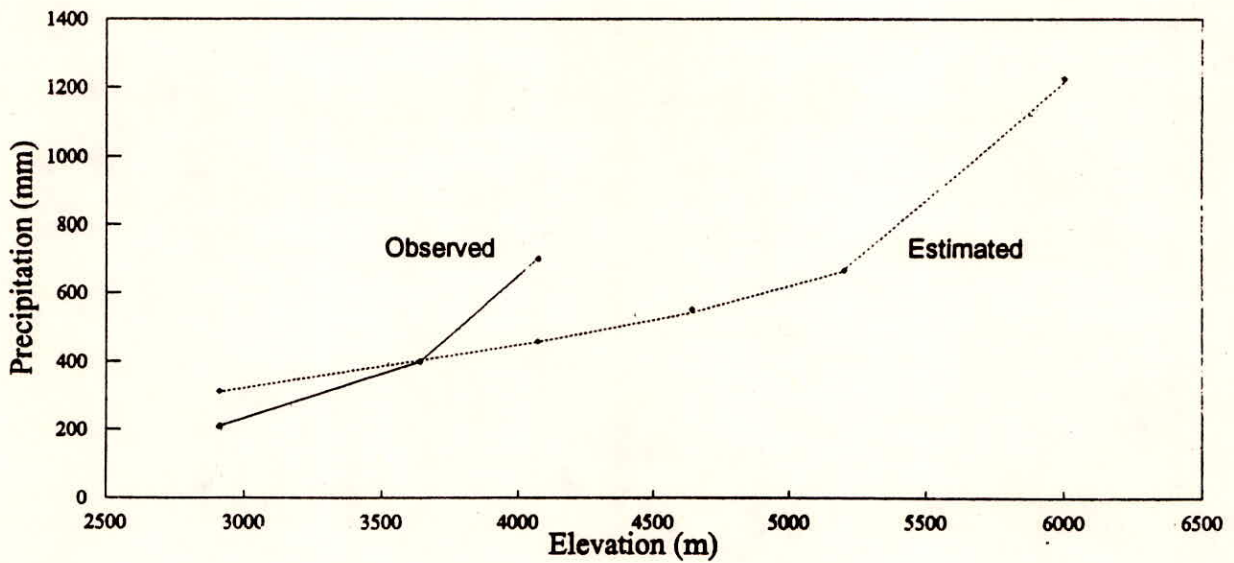Figure 2 : Variation in mean seasonal winter precipitation with elevation

224

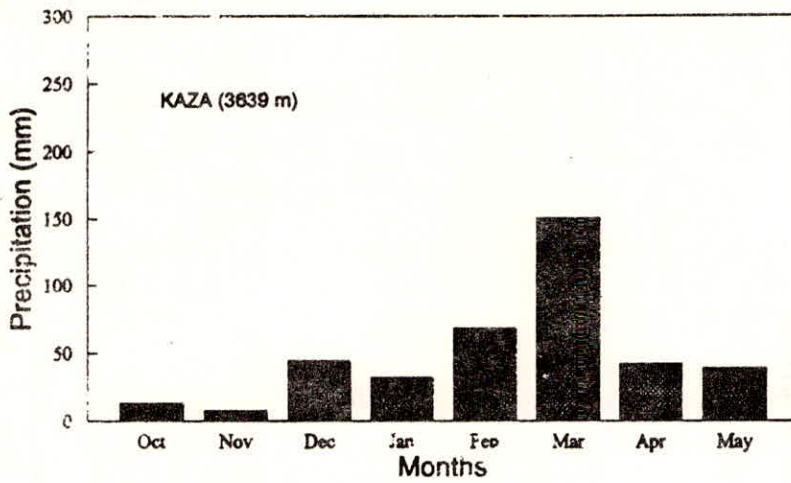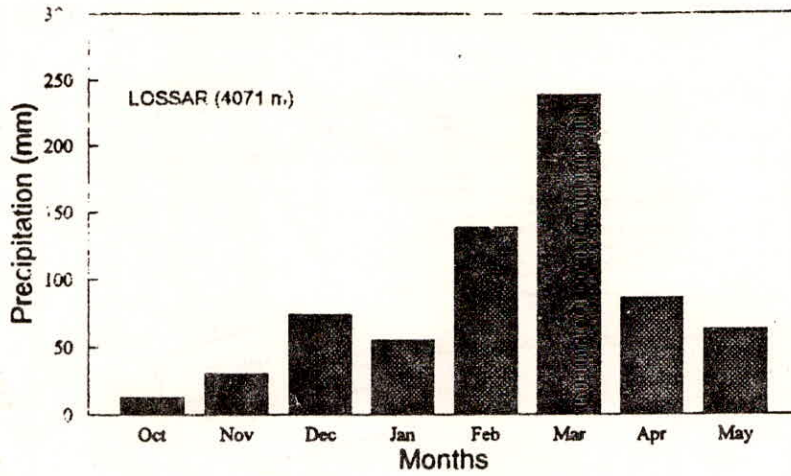Figure 3: Mean monthly precipitation distribution for the winter season.
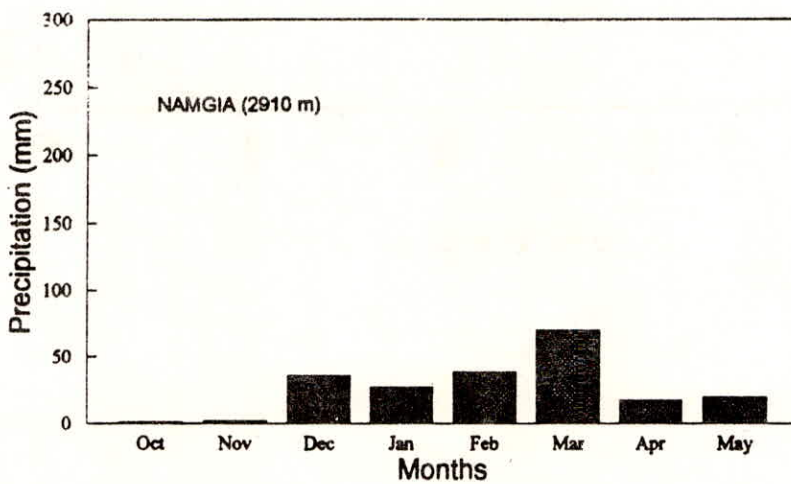
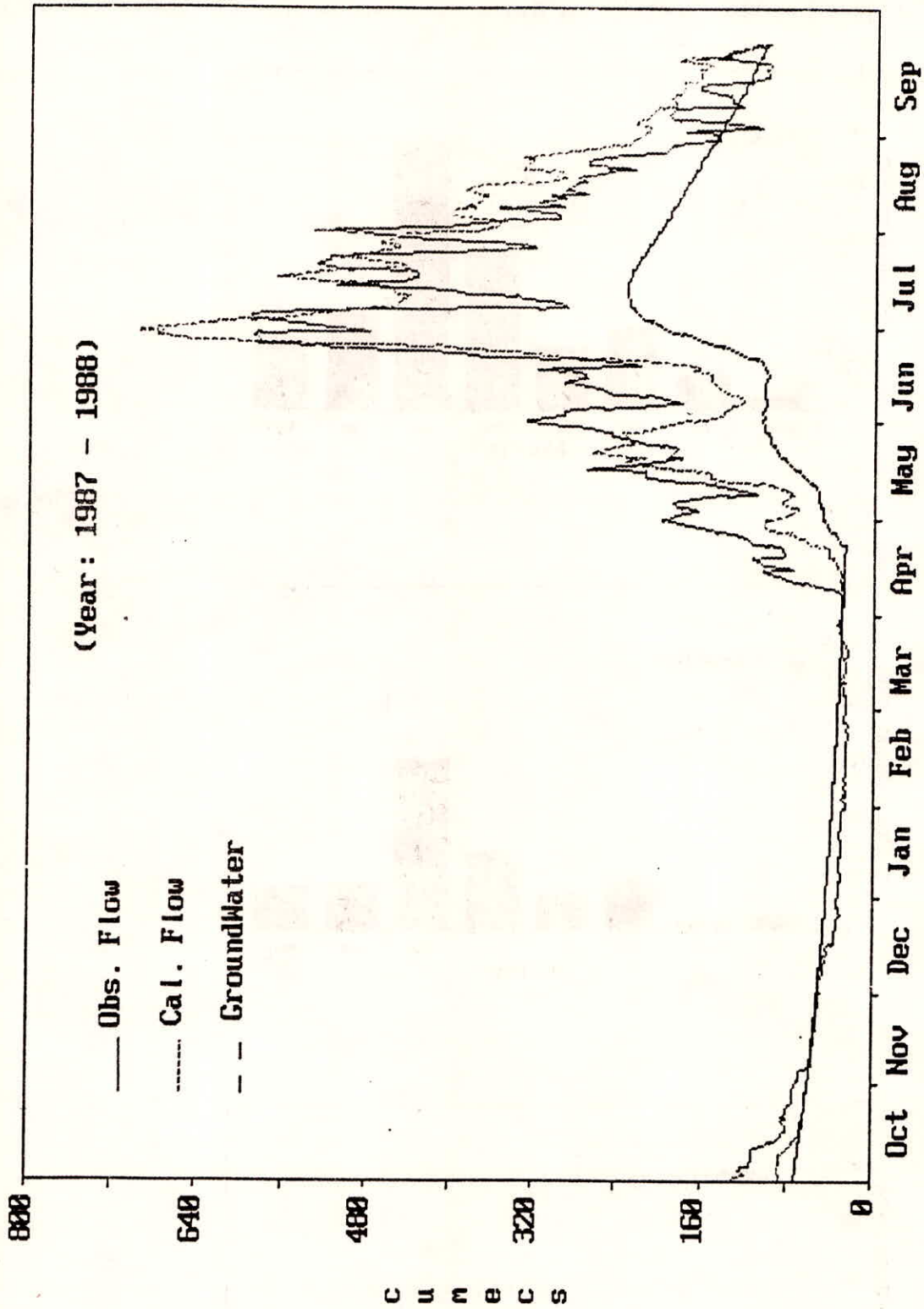Figure 4: Observed and computed streamflow for the year, 1987-88.

(Year : 1987 - 1988)

——— Obs. Flow
········ Cal. Flow
— — GroundWater

cumecs

800 640 480 320 160 0

Oct Nov Dec Jan Feb Mar Apr May Jun Jul Aug Sep

226

Figure 5. Observed and computed streamflow for the year, 1988-89.

(Year: 1988 - 1989)

—— Obs. Flow
······ Cal. Flow
– – GroundWater

cumecs

800 640 480 320 160 0

Oct Nov Dec Jan Feb Mar Apr May Jun Jul Aug Sep
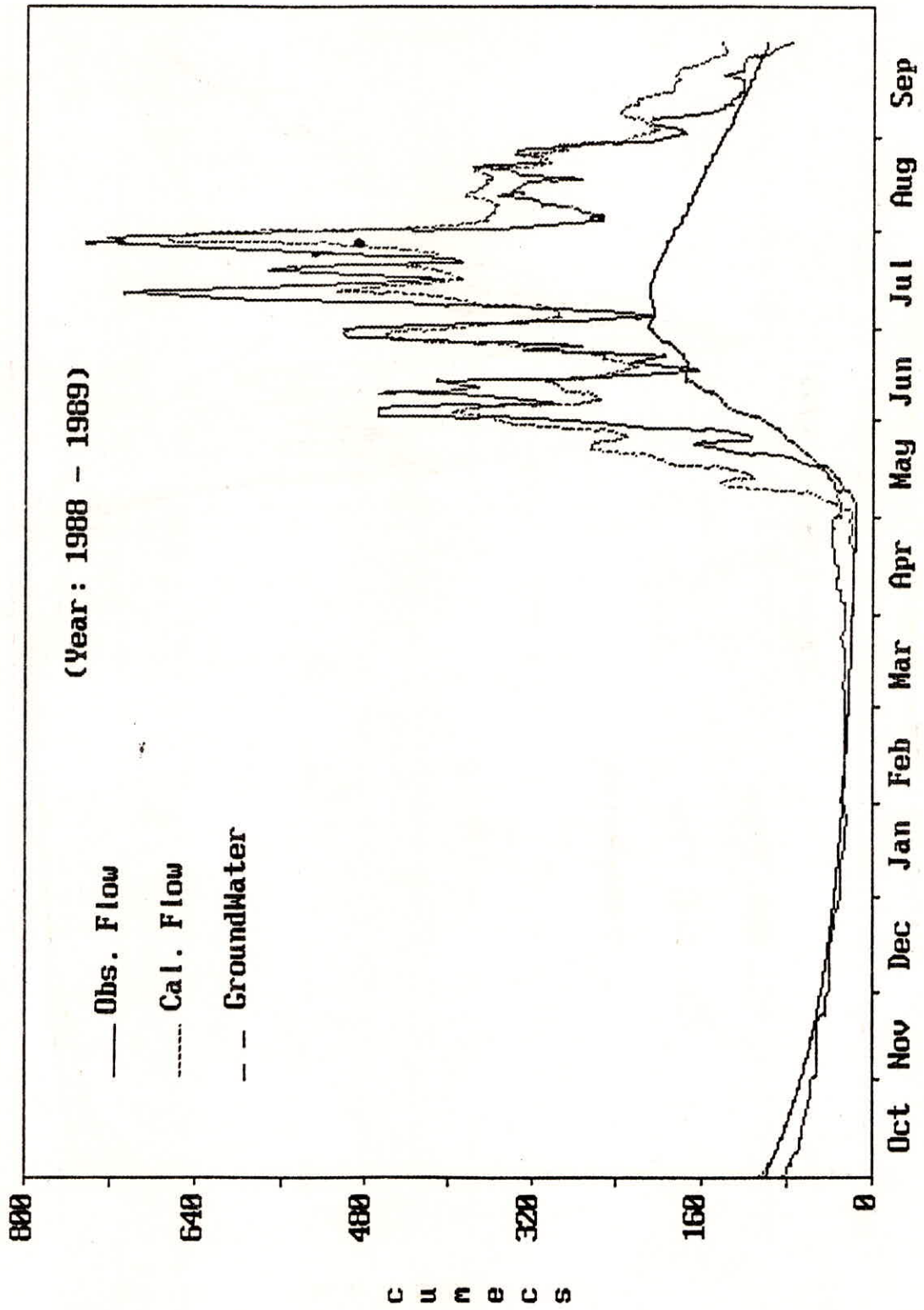
Figure 6: Observed and computed streamflow for the year, 1989--90.

(Year: 1989 - 1990)

—— Obs. Flow
...... Cal. Flow
-- GroundWater

Oct Nov Dec Jan Feb Mar Apr May Jun Jul Aug Sep

cumecs
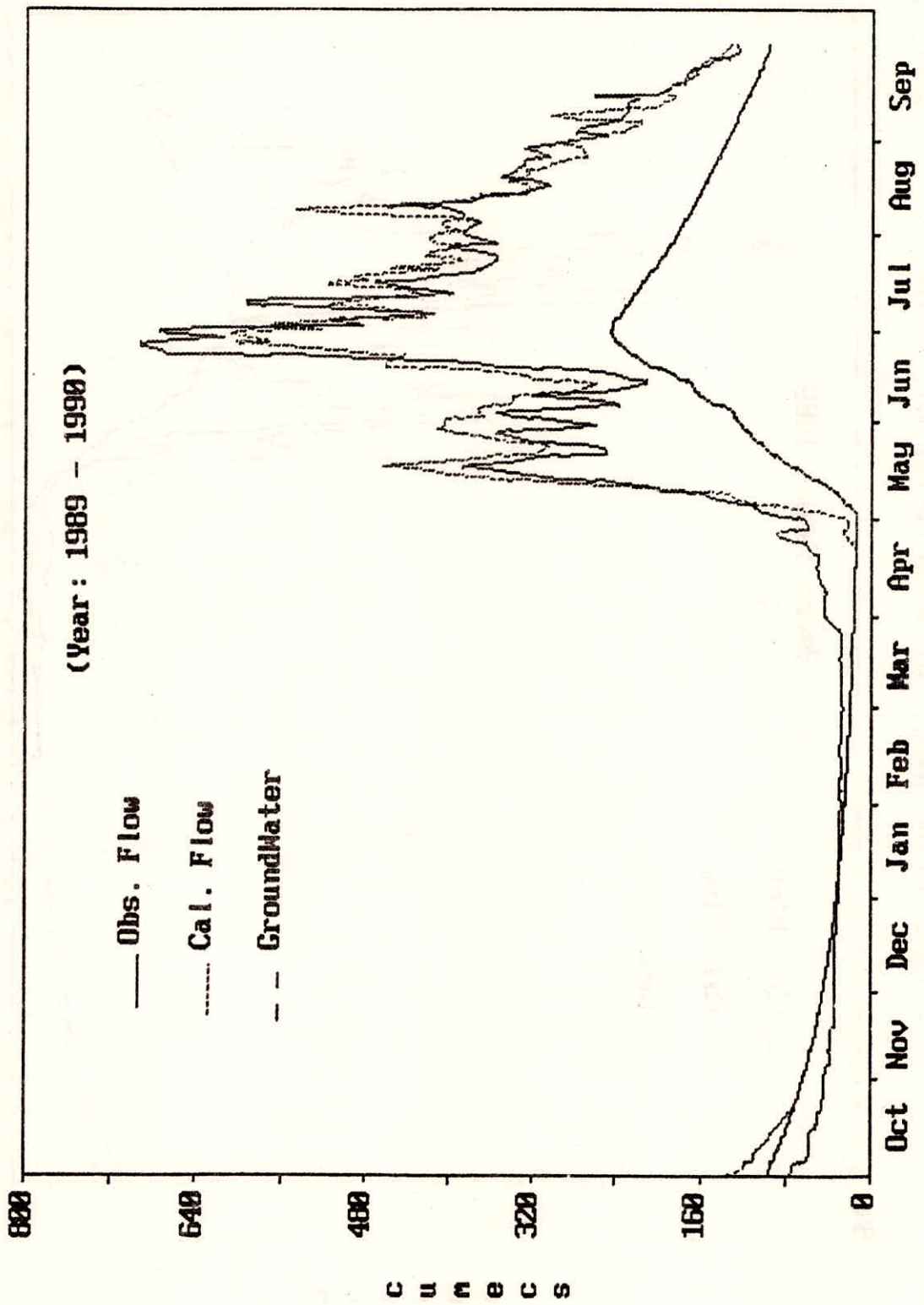
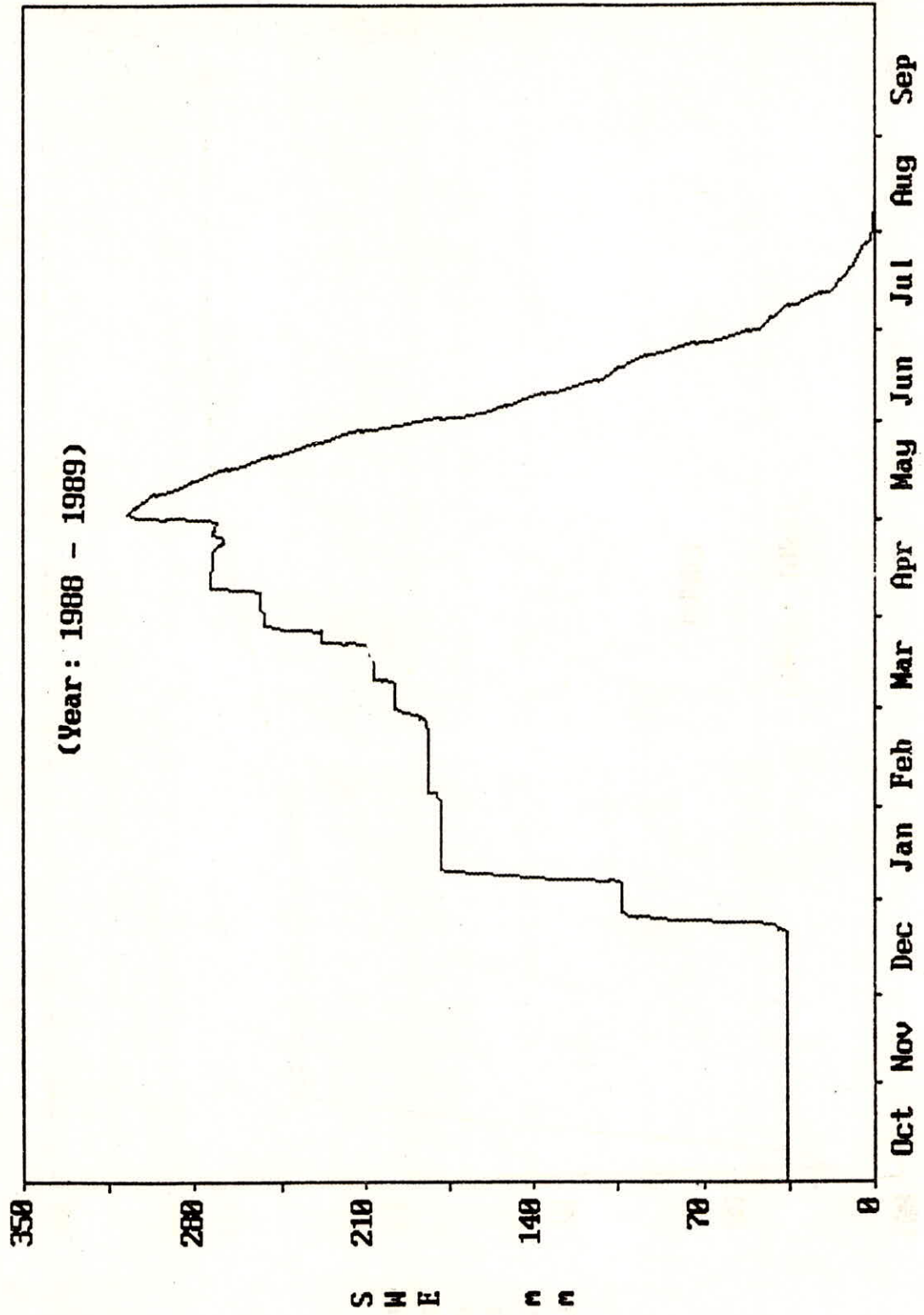Figure 7: Build-up and depletion of snow water equivalent for the year, 1988-89.

(Year: 1988 - 1989)

Figure 8: Changes in albedo with season.